Topological phase induced by distinguishing parameter regimes in a cavity optomechanical system with multiple mechanical resonators

Lu Qi,[1] Yan Xing,[1] Shutian Liu,[1,*] Shou Zhang,[1,2,†] and Hong-Fu Wang[2,‡]
[1]*School of Physics, Harbin Institute of Technology, Harbin, Heilongjiang 150001, China*
[2]*Department of Physics, College of Science, Yanbian University, Yanji, Jilin 133002, China*

(Received 17 December 2019; accepted 28 April 2020; published 15 May 2020)

We propose two kinds of distinguishing parameter regimes to induce a topological Su-Schrieffer-Heeger (SSH) phase in a one-dimensional (1D) multiresonator cavity optomechanical system via modulation of the frequencies of both cavity fields and resonators. The introduction of frequency modulations allows us to eliminate the Stokes heating process for mapping of the tight-binding Hamiltonian without the usual rotating-wave approximation, which is totally different from the traditional mapping of the topological tight-binding model. We find that the tight-binding Hamiltonian can be mapped into a topological SSH phase via modification of the Bessel function originating from the frequency modulations of cavity fields and resonators, and the induced SSH phase is independent of the effective optomechanical coupling strength. On the other hand, the insensitivity of the system to the effective optomechanical coupling provides us another new path to induce the topological SSH phase based on the present 1D cavity optomechanical system. And we show that the system can exhibit a topological SSH phase via variation of the effective optomechanical coupling strength in an alternative way, which is much easier to achieve in experiments. Furthermore, we also construct an analogous bosonic Kitaev model with trivial topology by keeping the Stokes heating processes. Our scheme provides a steerable platform for investigation of the effects of next-nearest-neighbor interactions on the topology of the system.

DOI: 10.1103/PhysRevA.101.052325

I. INTRODUCTION

Over the past decades, the cavity optomechanical system [1,2], which is composed of mechanical and optical modes, is becoming a fast-developing and appealing field for the investigation of fundamental quantum physics on the macroscopic scale. In the context of the optomechanical system, various questions have been explored, such as entanglement between mechanical modes and cavity fields [3–5], normal-mode splitting [6,7], optomechanical-induced transparency [8,9], squeezing of light or resonators [10–15], and cooling of resonators via feedback control [16]. Especially, more and more attention has been focused on modulated optomechanical systems [17–23] in recent years, for which abundant physical phenomena have been reported. A scheme of optomechanical cooling by utilization of the periodical modulations of frequency and damping of the resonator has been proposed [24]. Another cooling scheme of breaking the quantum backaction limit has also been proposed based on an optomechanical system by modulation of the frequencies of both the optical and the mechanical components [25], in which the Stokes heating processes can be safely and completely suppressed. The method of frequency modulation provides an effective path to eliminate the Stokes heating terms perfectly, which is essential to simulations of all kinds of topological matters.

The multiresonator cavity optomechanical system [26,27], as the assemblage of a set of single optomechanical systems, is also widely used to investigate diverse quantum questions [28–33]. de Moraes Neto *et al.* [34] designed a scheme for robust quantum-state transfer based on a one-dimensional (1D) optomechanical array by using the decoupling method. Akram *et al.* [35] proposed a scheme to achieve photon-phonon entanglement in coupled optomechanical arrays. Wan *et al.* [36] realized controllable photon and phonon localization induced by path interference in an optomechanical Lieb lattice. Simulations of the Z_2 topological insulator [37] and topological bosonic Majorana chains [38] have also been illustrated based on a 1D optomechanical array. Especially, in these previous studies, the derivation of the effective Hamiltonian in the optomechanical chain has mainly used the rotating-wave approximation to remove the Stokes heating processes. The topological Su-Schrieffer-Heeger (SSH) phase in a 1D multiresonator optomechanical system, in which the Stokes heating processes are eliminated via modulation of the frequencies of the cavity fields and resonators, has rarely been investigated to date.

In this paper, we propose a scheme to induce the topological SSH phase by dint of two different parameter regimes based on a 1D multiresonator cavity optomechanical system with time-dependent frequency modulations of both cavity fields and mechanical modes. We find that, after eliminating the Stokes heating terms via the Bessel function, the 1D tight-binding Hamiltonian can be obtained to induce a topological SSH phase. There exist two parameter regimes for inducing the SSH phase. One is the effective nearest-neighbor (NN)

*stliu@hit.edu.cn
†szhang@ybu.edu.cn
‡hfwang@ybu.edu.cn

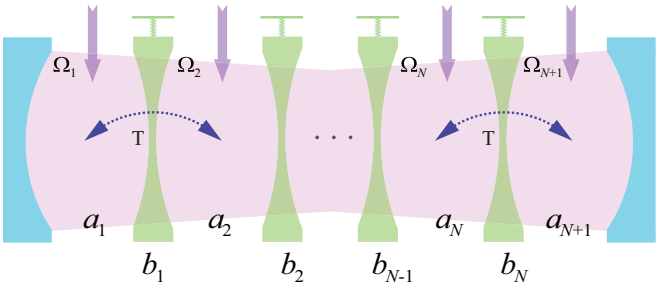

FIG. 1. Schematic of the 1D multiresonator optomechanical system, which contains $N+1$ cavity modes and N resonators. Each cavity mode is driven by a laser field and the coupling between resonator b_n and cavity field a_n (a_{n+1}) is g_n.

hopping strength, which is modulated to satisfy the staggered dimerized hopping strength of the SSH model by means of the Bessel function originating from frequency modulations. The other is the effective optomechanical coupling, which is varied alternately to induce a topological SSH phase after complete removal of the resonant Stokes heating processes. Furthermore, we also propose to build a bosonic Kitaev model based on the present 1D multiresonator cavity optomechanical system, in which the system possesses a continuous energy spectrum corresponding to the arbitrary strength of analogous pairing terms. In addition, we find that the next-nearest-neighbor (NNN) interactions between two adjacent cavity fields can be flexibly adjusted and even completely suppressed, which provides a novel and controllable platform for investigation of the effect of NNN hopping on the topology of the system.

The paper is organized as follows: In Sec. II, we derive the effective linearized Hamiltonian of the 1D multiresonator optomechanical system with time-dependent frequency modulations. In Sec. III, we remove the Stocks heating terms from the Hamiltonian and induce a topological SSH phase via two different kinds of parameter regimes. Subsequently, an analogous bosonic Kitaev model is obtained via frequency modulations. Also, we investigate the effect of NNN hopping on the topology of the system. Finally, a conclusion is given in Sec. IV.

II. SYSTEM AND HAMILTONIAN

Consider a 1D multiresonator cavity optomechanical system composed of $N+1$ cavity fields and N resonators, in which the frequencies of the cavity fields and resonators can be modulated, as shown in Fig. 1. In this array, each cavity field is driven by a laser with frequency $\omega_{d,n}$ and strength Ω_n. The two adjacent cavity fields possess direct coupling with hopping strength T and the single-phonon optomechanical coupling strength between resonator b_n and cavity field a_n (a_{n+1}) is g_n. In this way the system is dominated by the Hamiltonian

$$\begin{aligned} H =& \sum_{n=1}^{N+1}[\omega_{a,n}+\lambda_n\nu\cos(\nu t+\phi)]a_n^\dagger a_n \\ &+\sum_{n=1}^{N}[\omega_{b,n}+\gamma_n\nu\cos(\nu t+\phi)]b_n^\dagger b_n \\ &+\sum_{n=1}^{N+1}(\Omega_n a_n^\dagger e^{-i\omega_{d,n}t}+\Omega_n^* a_n e^{i\omega_{d,n}t}) \\ &-\sum_{n=1}^{N} g_n(a_n^\dagger a_n - a_{n+1}^\dagger a_{n+1})(b_n^\dagger + b_n) \\ &+\sum_{n=1}^{N} T(a_{n+1}^\dagger a_n + a_n^\dagger a_{n+1}), \end{aligned} \tag{1}$$

where $a_n^\dagger$ ($b_n^\dagger$) is the creation operator of the optical cavity field (mechanical resonator) and a_n (b_n) is its corresponding annihilation operator. The first two terms represent the modulated free energy of cavity fields and resonators with the modulated strength λ_n (γ_n), frequency ν, and phase ϕ. The frequency modulations of the cavity field and resonator can be realized experimentally via a laser irradiated onto the cavity field [39] and a gate electrode applied on the resonator [40], respectively. The third term describes the interaction between the cavity field and the external driving laser field. The fourth term represents the interaction between the cavity field a_n (a_{n+1}) and the mechanical resonator b_n. And the last term denotes the direct interaction between two adjacent cavity fields.

Under the condition of strong laser driving, we choose to work in a rotating frame with respect to the driving frequency and rewrite the operators as $a_n = \alpha_n + \delta a_n$ ($b_n = \beta_n + \delta b_n$). After dropping the notation δ for all the fluctuation operators δa_n (δb_n), the Hamiltonian is given by

$$\begin{aligned} H_L =& \sum_{n=1}^{N+1}[\Delta'_{a,n}+\lambda_n\nu\cos(\nu t+\phi)]a_n^\dagger a_n \\ &+\sum_{n=1}^{N}[\omega_{b,n}+\gamma_n\nu\cos(\nu t+\phi)]b_n^\dagger b_n \\ &-\sum_{n=1}^{N} g_n(\alpha_n^* a_n + \alpha_n a_n^\dagger \\ &-\alpha_{n+1}^* a_{n+1} - \alpha_{n+1} a_{n+1}^\dagger)(b_n^\dagger + b_n) \\ &+\sum_{n=1}^{N} T(a_{n+1}^\dagger a_n + a_n^\dagger a_{n+1}), \end{aligned} \tag{2}$$

where $\Delta'_{a,n}$ is the effective detuning originating from optomechanical coupling with $\Delta'_{a,1} = \Delta_{a,1} - g_1[\beta_1^* + \beta_1]$, $\Delta'_{a,N+1} = \Delta_{a,N+1} + g_N[\beta_N^* + \beta_N]$, and $\Delta'_{a,n=2\ldots N} = \Delta_{a,n} + g_{n-1}(\beta_{n-1}^* + \beta_{n-1}) - g_n(\beta_n^* + \beta_n)$, and $\Delta_{a,n} = \omega_{a,n} - \omega_{d,n}$ is the detuning between cavity fields and driving fields. We stress that effective detuning $\Delta'_{a,n}$ satisfies $\Delta'_{a,n} \approx \Delta_{a,n}$ due to the existence of the extremely weak optomechanical coupling. Thus, under the red-detuning regime with $\Delta'_{a,n} \approx \Delta_{a,n} = \omega_{b,n}$, the system may reach steady state accompanied by the final periodically time-dependent steady cavity field α_n due to the existence of the periodically time-dependent frequency of the cavity field and resonator (see Appendix A for more discussion). The steady-state dynamics of the present optomechanical system is the basis for investigation of various quantum optical issues. To clarify it further, we perform the

rotating transformation defined by

$$V = \exp\left\{\sum_{n=1}^{N+1} -i\Delta'_{a,n}t a_n^\dagger a_n - i\lambda_n \sin(\nu t+\phi) a_n^\dagger a_n + \sum_{n=1}^{N} -i\omega_{b,n}t b_n^\dagger b_n - i\gamma_n \sin(\nu t+\phi) b_n^\dagger b_n\right\}. \quad (3)$$

After this, the Hamiltonian becomes

$$\begin{aligned} H'_L = \sum_n \{ & -G_n a_n^\dagger b_n e^{i[(\Delta'_{a,n}-\omega_{b,n})t+(\lambda_n-\gamma_n)\sin(\nu t+\phi)]} \\ & - G_n a_n^\dagger b_n^\dagger e^{i[(\Delta'_{a,n}+\omega_{b,n})t+(\lambda_n+\gamma_n)\sin(\nu t+\phi)]} \\ & + G_{n+1} a_{n+1}^\dagger b_n e^{i[(\Delta'_{a,n+1}-\omega_{b,n})t+(\lambda_{n+1}-\gamma_n)\sin(\nu t+\phi)]} \\ & + G_{n+1} a_{n+1}^\dagger b_n^\dagger e^{i[(\Delta'_{a,n+1}+\omega_{b,n})t+(\lambda_{n+1}+\gamma_n)\sin(\nu t+\phi)]} \\ & + T a_{n+1}^\dagger a_n e^{i(\lambda_{n+1}-\lambda_n)\sin(\nu t+\phi)}\} + \text{H.c.}, \end{aligned} \quad (4)$$

where the first and third terms represent the anti-Stokes terms for cooling of the resonators, the second and fourth terms describe the Stokes heating processes of the resonators, and $G_n = g_n\alpha_n$ ($G_{n+1} = g_n\alpha_{n+1}$) is the effective optomechanical coupling. The Stokes heating terms of the resonators are usually useless to the system, which means that the Stokes heating terms should be removed via diverse parameter regimes. Apparently, the existence of frequency modulations of the cavity fields and resonators may provide us a new way to deal with the Stokes heating terms. At the same time, note that the entire above derivation is based on an optomechanical system with $N+1$ cavity fields and N resonators. We stress that an optomechanical system with N cavity fields and N resonators has a similar final effective Hamiltonian (see Appendix B for the case of N cavity fields and N resonators), which means that our scheme is also valid for an optomechanical system with N cavity fields and N resonators.

III. TOPOLOGICAL PHASE AND PHASE TRANSITION INDUCED BY DIFFERENT PARAMETER REGIMES

The crucial issue in the process of inducing an usual topological phase is to derive the tight-binding Hamiltonian, which implies that the Stokes heating terms should be eliminated. In Sec. III A below we use the frequency modulations to remove the Stokes heating terms and induce a topological SSH phase in terms of two different parameter regimes.

A. Topological SSH phases induced by frequency modulations

To obtain the necessary tight-binding Hamiltonian for simulation of the standard SSH model, we consider the case where the system does not possess direct coupling between two adjacent cavity fields ($T = 0$) and take the phase of frequency modulations as $\phi = 0$. After performance of the Jacobi-Anger expansions $e^{i\kappa\sin\nu t} = \sum_{m=-\infty}^{\infty} J_m(\kappa)e^{im\nu t}$, the Hamiltonian in Eq. (4) can be rewritten as

$$\begin{aligned} H_{L,A_1} = \sum_n \Bigg\{ & -\sum_{m_1=-\infty}^{\infty} G_n J_{m_1}(\kappa_{1,n}) a_n^\dagger b_n e^{i[(\Delta'_{a,n}-\omega_{b,n})+m_1\nu]t} - \sum_{m_2=-\infty}^{\infty} G_n J_{m_2}(\kappa_{2,n}) a_n^\dagger b_n^\dagger e^{i[(\Delta'_{a,n}+\omega_{b,n})+m_2\nu]t} \\ & + \sum_{m_3=-\infty}^{\infty} G_{n+1} J_{m_3}(\kappa_{3,n}) a_{n+1}^\dagger b_n e^{i[(\Delta'_{a,n+1}-\omega_{b,n})+m_3\nu]t} + \sum_{m_4=-\infty}^{\infty} G_{n+1} J_{m_4}(\kappa_{4,n}) a_{n+1}^\dagger b_n^\dagger e^{i[(\Delta'_{a,n+1}+\omega_{b,n})+m_4\nu]t} \Bigg\} + \text{H.c.}, \end{aligned} \quad (5)$$

where $\kappa_{1,n} = \lambda_n - \gamma_n$, $\kappa_{2,n} = \lambda_n + \gamma_n$, $\kappa_{3,n} = \lambda_{n+1} - \gamma_n$, $\kappa_{4,n} = \lambda_{n+1} + \gamma_n$, and $J_{m_j}(\kappa_{j,n})$ is the m_jth order of the first kind of Bessel function with $j = 1, 2, 3, 4$.

When the frequency modulation parameters satisfy $\Delta'_{a,n} = \Delta'_{a,n+1} = \omega_{b,n}$, $\nu = \omega_{b,n}$ (see Appendix C for the rationale), $m_1 = m_3 = 0$, and $m_2 = m_4 = -2$, we find that the system possesses resonant anti-Stokes terms and Stokes heating terms simultaneously. Then the Hamiltonian in Eq. (5) becomes

$$\begin{aligned} H_{L,A_2} = \sum_n \{ & -G_n J_0(\kappa_{1,n}) a_n^\dagger b_n - G_n J_{-2}(\kappa_{2,n}) a_n^\dagger b_n^\dagger \\ & + G_{n+1} J_0(\kappa_{3,n}) a_{n+1}^\dagger b_n + G_{n+1} J_{-2}(\kappa_{4,n}) a_{n+1}^\dagger b_n^\dagger\} + \text{H.c.} \end{aligned} \quad (6)$$

Obviously, the resonant Stokes heating terms in Eq. (6) are useless in the usual mapping of the tight-binding Hamiltonian. In previous investigations with respect to mapping of the bosonic topological tight-binding Hamiltonian, the Stokes heating terms have been removed mainly by use of the rotating-wave approximation [37,41,42]. Here we apply the frequency modulation method to deal with the Stokes heating processes. By choosing the Bessel coefficients to satisfy $J_{-2}(\kappa_{2,n}) = J_{-3}(\kappa_{4,n}) = 0$, the Stokes heating terms can be suppressed and even eliminated completely, and the tight-binding Hamiltonian is expressed as

$$H_{L,A} = \sum_n [-G_n J_0(\kappa_{1,n}) a_n^\dagger b_n + G_{n+1} J_0(\kappa_{3,n}) a_{n+1}^\dagger b_n] + \text{H.c.} \quad (7)$$

Obviously, the above Hamiltonian is equivalent to an SSH-type Hamiltonian if we map the cavity field a_n and resonator b_n as two sites of the SSH model. Theoretically, the condition $J_{-2}(\kappa_{2,n}) = J_{-2}(\kappa_{4,n}) = 0$ can be easily achieved by choosing the parameters to satisfy $\kappa_{2,n} \sim \infty$, $\kappa_{4,n} \sim \infty$, and $\kappa_{2,n} \approx \kappa_{4,n}$. In experiments, we can choose frequency modulations strong enough to make the Bessel coefficients satisfy $J_{-2}(\kappa_{2,n}) = J_{-2}(\kappa_{4,n}) = 0$ approximately. Previous investigations on induction of a topological phase based on the 1D multiresonator optomechanical system have mainly depended on the periodic modulation of the effective optomechanical coupling strength [37]. We here propose a new way to induce a topological SSH phase via the Bessel function originating from the frequency modulations of cavity fields and resonators. The condition of strong enough frequency modulations ($\kappa_{2,n} \approx \kappa_{4,n} \sim \infty$)

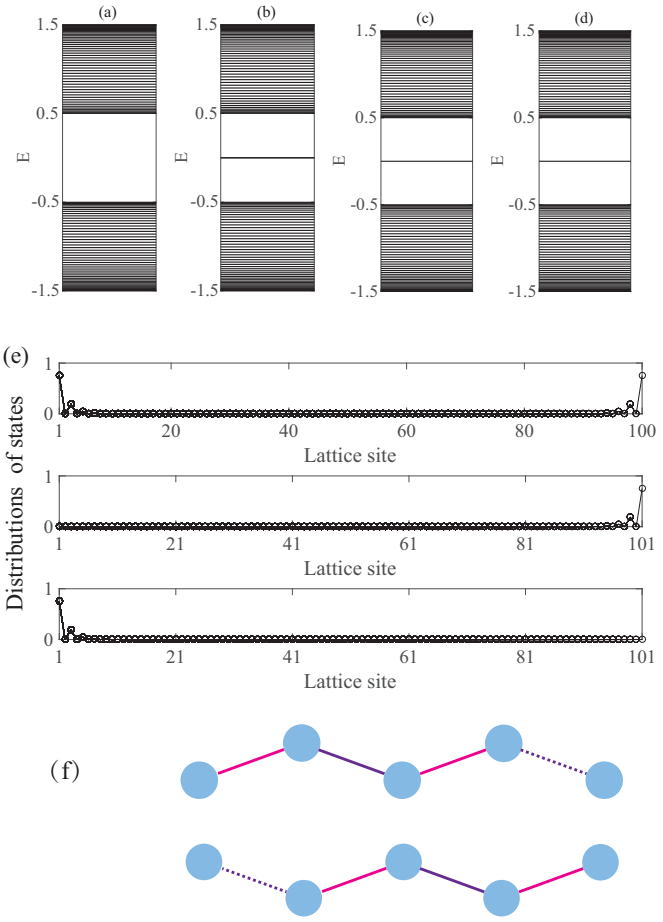

FIG. 2. Energy spectra and distributions of edge states. (a) Energy spectrum corresponding to $J_0(\kappa_{1,n}) > J_0(\kappa_{3,n})$; the size of the cavity optomechanical lattice chain system is $L = 100$. (b) Energy spectrum corresponding to $J_0(\kappa_{1,n}) < J_0(\kappa_{3,n})$, $L = 100$. (c) Energy spectrum corresponding to $J_0(\kappa_{1,n}) > J_0(\kappa_{3,n})$, $L = 101$. (d) Energy spectrum corresponding to $J_0(\kappa_{1,n}) < J_0(\kappa_{3,n})$, $L = 101$. (e) Distributions of edge states in (b)–(d). (f) Schematic of the odd-even effect of the SSH chain. Red, purple, and dashed lines represent strong hopping bonds, weak hopping bonds, and decoupling of the edge site, respectively. When the size of the cavity optomechanical lattice chain system is an odd number, the last site will decouple from the lattice chain when $-G_n J_{-1}(\kappa_{1,n}) > G_{n+1} J_{-1}(\kappa_{3,n})$ and the first site will separate from the lattice chain when $-G_n J_{-1}(\kappa_{1,n}) < G_{n+1} J_{-1}(\kappa_{3,n})$. Other parameters are taken as $-G_n = G_{n+1}$.

means that the other two Bessel parameters should satisfy $\kappa_{1,n} \neq \kappa_{3,n}$. Thus we can obtain different values of the zeroth Bessel function [such as $J_0(\kappa_{1,n}) < J_0(\kappa_{3,n})$ or $J_0(\kappa_{1,n}) > J_0(\kappa_{3,n})$] by choosing different values of $\kappa_{1,n}$ and $\kappa_{3,n}$. To emphasize the impact of the Bessel coefficients $J_0(\kappa_{1,n})$ and $J_0(\kappa_{3,n})$, we take the effective optomechanical coupling strength to satisfy $-G_n = G_{n+1}$ (see Appendix D for more discussion). Then the topological properties of the system can be identified by the values of $J_0(\kappa_{1,n})$ and $J_0(\kappa_{3,n})$. When the Bessel function is chosen to satisfy $J_0(\kappa_{1,n}) > J_0(\kappa_{3,n})$, the multiresonator optomechanical system exhibits a topologically trivial phase corresponding to a lattice chain with an even number of sites, as illustrated in Fig. 2(a). Conversely, when it satisfies $J_0(\kappa_{1,n}) < J_0(\kappa_{3,n})$, the system possesses two degenerate edge states located at both ends of the system with an even number of sites, as shown in Fig. 2(b). For the case where the size of the multiresonator optomechanical system is taken as an odd number, we find that the system possesses an edge state located at the rightmost end $[J_0(\kappa_{1,n}) > J_0(\kappa_{3,n})]$ or the leftmost end $[J_0(\kappa_{1,n}) < J_0(\kappa_{3,n})]$ of the optomechanical array, which is induced by the odd-even effect of the SSH model, as shown in Figs. 2(c) and 2(d). To further clarify the topological edge states, we plot the distributions of edge states corresponding to an even-number and an odd-number lattice size, respectively, as shown in Fig. 2(e). Also, a schematic of the odd-even effect of the SSH chain is depicted in Fig. 2(f).

We should stress that the topological SSH phase can also be induced corresponding to $-G_n \neq G_{n+1}$ and even with $-G_n > G_{n+1}$. Due to the selectivity of the values of the Bessel function, we can always find a set of $J_0(\kappa_{1,n})$ and $J_0(\kappa_{3,n})$ to make the effective hopping parameters between an adjacent cavity field and the resonator satisfy $-G_n J_0(\kappa_{1,n}) < G_{n+1} J_0(\kappa_{3,n})$ in a certain range even when $-G_n > G_{n+1}$. This weak-strong alternating effective hopping strength is the crucial condition for induction of the SSH phase. Apparently, the method we use to induce the SSH phase is independent of the effective optomechancal coupling strength. The insensitivity of the present scheme to the optomechancal coupling strength provides a new path to induction of a topological SSH phase in the 1D multiresonator optomechanical system. Meanwhile, we clarify that this method requires strong enough frequency modulations, which may cause certain difficulties in experiments. In order to avoid this obstacle in the experimental simulation of a nontrivial SSH phase based on the present cavity optomechanical system, in Sec. III B we propose another parameter regime to induce the SSH phase.

B. Topological SSH phases induced via strong effective optomechanical coupling

Here we propose how to eliminate the resonant Stokes heating terms using the effective optomechanical coupling parameter regime and show that the topological phase can be induced successfully and effectively. Choosing the modulation strengths of the cavity field and resonator to satisfy $\lambda_{n+1} = \lambda_n = \gamma_n$ and $T = \phi = 0$, the Hamiltonian in Eq. (4) becomes

$$H_{L,B_1} = \sum_n \{-G_n a_n^\dagger b_n e^{i(\Delta'_{a,n} - \omega_{b,n})t} - G_n a_n^\dagger b_n^\dagger e^{i[(\Delta'_{a,n} + \omega_{b,n})t + 2\lambda_n \sin(\nu t)]} + G_{n+1} a_{n+1}^\dagger b_n e^{i(\Delta'_{a,n+1} - \omega_{b,n})t}$$
$$+ G_{n+1} a_{n+1}^\dagger b_n^\dagger e^{i[(\Delta'_{a,n+1} + \omega_{b,n})t + (\lambda_{n+1} + \lambda_n)\sin(\nu t)]}\} + \text{H.c.} \quad (8)$$

After exploiting the Jacobi-Anger expansions, the Hamiltonian is expressed as

$$H_{L,B_2} = \sum_n \Bigg\{ -G_n a_n^\dagger b_n e^{i(\Delta'_{a,n}-\omega_{b,n})t} + G_{n+1} a_{n+1}^\dagger b_n e^{i(\Delta'_{a,n+1}-\omega_{b,n})t} + \sum_{m_1=-\infty}^{\infty} -G_n J_{m_1}(\kappa_{1,n}) a_n^\dagger b_n^\dagger e^{i[(\Delta'_{a,n}+\omega_{b,n})+m_1\nu]t} + \sum_{m_2=-\infty}^{\infty} G_{n+1} J_{m_2}(\kappa_{2,n}) a_{n+1}^\dagger b_n^\dagger e^{i[(\Delta'_{a,n+1}+\omega_{b,n})+m_2\nu]t} \Bigg\} + \text{H.c.}, \tag{9}$$

where $\kappa_{1,n} = 2\lambda_n$ and $\kappa_{2,n} = \lambda_{n+1} + \lambda_n$. Under the red-detuning regime of $\Delta'_{a,n} = \Delta'_{a,n+1} = \omega_{b,n}$, the time-dependent exponential in NN hopping terms can be removed safely, and the Hamiltonian can be rewritten as

$$H_{L,B_3} = \sum_n \left[-G_n a_n^\dagger b_n + G_{n+1} a_{n+1}^\dagger b_n + \sum_{m_1=-\infty}^{\infty} -G_n J_{m_1}(\kappa_{1,n}) a_n^\dagger b_n^\dagger e^{i(2\omega_{b,n}+m_1\nu)t} + \sum_{m_2=-\infty}^{\infty} G_{n+1} J_{m_2}(\kappa_{2,n}) a_{n+1}^\dagger b_n^\dagger e^{i(2\omega_{b,n}+m_2\nu)t} \right] + \text{H.c.} \tag{10}$$

Thus the system has resonant Stokes heating terms when $\nu = \omega_{b,n}$ and $m_1 = m_2 = -2$, leading to

$$H_{L,B_4} = \sum_n [-G_n a_n^\dagger b_n + G_{n+1} a_{n+1}^\dagger b_n - G_n J_{-2}(\kappa_{1,n}) a_n^\dagger b_n^\dagger + G_{n+1} J_{-2}(\kappa_{2,n}) a_{n+1}^\dagger b_n^\dagger] + \text{H.c.} \tag{11}$$

Apparently, we can safely remove the resonant Stokes heating terms by choosing appropriate values of $\kappa_{1,n}$ and $\kappa_{2,n}$ to satisfy $J_{-2}(\kappa_{1,n}) = J_{-2}(\kappa_{2,n}) = 0$. We stress that the process of eliminating Stokes heating terms does not involve the rotating-wave approximation. Thus this method provides a new way to obtain the tight-binding Hamiltonian for inducing a topological phase based on the present optomechanical system with frequency modulations. Another advantage is that the effective optomechanical coupling G_n (G_{n+1}) can realize the strong-coupling regime, in which the couplings between the resonator and the adjacent cavity fields can be selected over a wider range. Then the system can be described by the following tight-binding SSH Hamiltonian:

$$H_{L,B} = \sum_n [-G_n a_n^\dagger b_n + G_{n+1} a_{n+1}^\dagger b_n] + \text{H.c.} \tag{12}$$

Based on this Hamiltonian, the topologically nontrivial SSH phase can be obtained by varying the adjacent effective optomechanical coupling strength in an alternative way, such as $-G_n < G_{n+1}$.

C. Topologically trivial Kitaev model

Here, we induce an analogous Kitaev Hamiltonian using the frequency modulations of cavity fields and resonators in the 1D multiresonator optomechanical system. Consider the parameter regime $\lambda_{n+1} = \lambda_n = \gamma_n$, $\phi \neq 0$, and $T = 0$; after performing the Jacobi-Anger transformation under the red-detuning regime again, the Hamiltonian of the system can be derived as

$$H_{L,C_1} = \sum_n \Bigg[-G_n a_n^\dagger b_n + G_{n+1} a_{n+1}^\dagger b_n. + \sum_{m_1=-\infty}^{\infty} -G_n J_{m_1}(\kappa_{1,n}) a_n^\dagger b_n^\dagger e^{i(2\omega_b+m_1\nu)t} e^{im_1\phi} + \sum_{m_2=-\infty}^{\infty} G_{n+1} J_{m_2}(\kappa_{2,n}) a_{n+1}^\dagger b_n^\dagger e^{i(2\omega_b+m_2\nu)t} e^{im_2\phi} \Bigg] + \text{H.c.} \tag{13}$$

The resonant Stokes heating terms can be obtained by choosing $m_1 = m_2 = -2$. With the choice of $\phi = -0.25\pi$, the Hamiltonian becomes

$$H_{L,C_2} = \sum_n [-G_n a_n^\dagger b_n + G_{n+1} a_{n+1}^\dagger b_n - iG_n J_{-2}(\kappa_{1,n}) a_n^\dagger b_n^\dagger + iG_{n+1} J_{-2}(\kappa_{2,n}) a_{n+1}^\dagger b_n^\dagger] + \text{H.c.} \tag{14}$$

For mapping of the Kitaev model Hamiltonian, we choose the effective optomechanical coupling strength to satisfy $-G_n = G_{n+1} = G_c$ (a fixed value). After this, the Hamiltonian becomes

$$H_{L,C} = \sum_n [G_c a_n^\dagger b_n + G_c a_{n+1}^\dagger b_n + iG_c J_{-2}(\kappa_{1,n}) a_n^\dagger b_n^\dagger + iG_c J_{-2}(\kappa_{2,n}) a_{n+1}^\dagger b_n^\dagger] + \text{H.c.} \tag{15}$$

One can clearly see that the form of the above Hamiltonian is identical to that of the Kitaev model with zero chemical potential, in which the first two terms represent the NN hopping and the imaginary Stokes heating terms are analogous to the superconducting pairing terms of the Kitaev model. We simulate the energy spectra of the standard fermionic Kitaev model and the present cavity optomechanical lattice chain system numerically, as shown in Figs. 3(a) and 3(b). Compared to the standard fermionic Kitaev model, we find that the present system only possesses a continuous nongapped energy spectrum corresponding to arbitrary values of $J_{-2}(\kappa_{1,n})$ and $J_{-2}(\kappa_{2,n})$, which is significantly different from the fermionic Kitaev energy spectrum, exhibiting two degenerate zero-energy modes in the gap. The reason is that the bosonic operators satisfy the commutation relation, which means that by simply replacing the fermionic operators in the standard Kitaev model with the bosonic operators, one cannot obtain the same Majorana double-chain structure as in the fermionic Kitaev model [43]. Therefore, the present bosonic Kitaev Hamiltonian with the same real-space form as in the

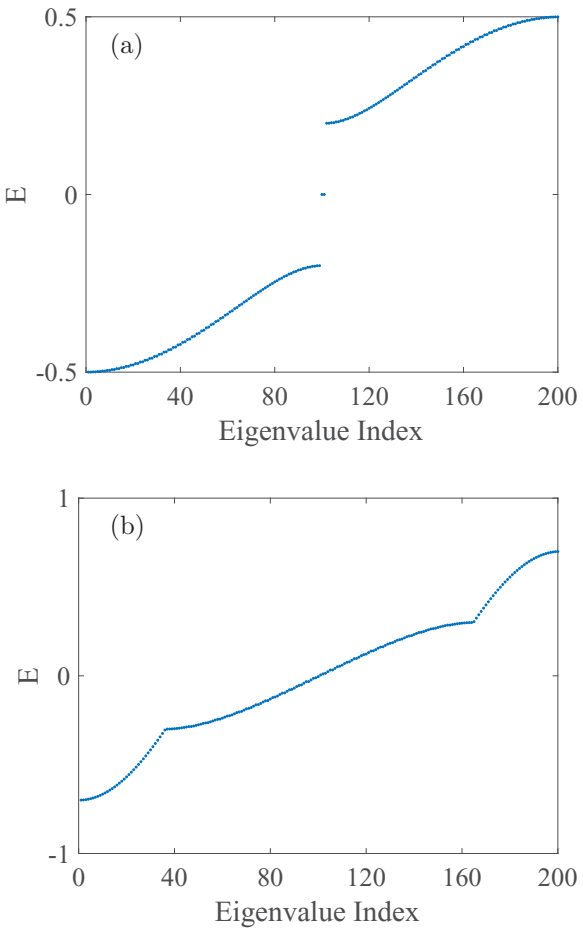

FIG. 3. Energy spectra ($2L$ eigenvalues) of the system under Majorana representation. (a) Standard Kitaev energy spectrum when the system satisfies Fermi exchange antisymmetry [$G_c = 0.5$, $G_c J_{-2}(\kappa_{1,n}) = G_c J_{-2}(\kappa_{2,n}) = 0.2$]. (b) Kitaev energy spectrum of the present system, which does not satisfy Fermi exchange antisymmetry [$G_c = 0.5$, $G_c J_{-2}(\kappa_{1,n}) = G_c J_{-2}(\kappa_{2,n}) = 0.2$]. The size of the system is $L = 100$.

fermionic Kitaev model exhibits trivial topology and has a nongapped energy spectrum.

D. Effects of partial next-nearest-neighbor hopping regulated by frequency modulations

The interaction between two adjacent cavity fields is not taken into account in the above discussion. However, a realistic cavity optomechanical system may possess a strong direct coupling between cavity fields, which corresponds to partial NNN hopping in the perspective of mapping the cavity field a_n and resonator b_n as two sites in the SSH model. In this way, the direct coupling between two cavity fields is equivalent to the NNN hopping only added onto the odd sites of the SSH chain. In the following we discuss the effects of partial NNN hopping on the system by choosing the parameters of frequency modulations to satisfy $\lambda_{n+1} = \lambda_n = \gamma_n$, $\phi = 0$, and $T \neq 0$. After removal of the Stokes heating terms as discussed in Sec. III B, the system can be dominated by the tight-binding Hamiltonian

$$H_{L,D_1} = \sum_n \Big[-G_n a_n^\dagger b_n + G_{n+1} a_{n+1}^\dagger b_n + \sum_{m=-\infty}^{\infty} T J_m(\kappa_{1,n}) a_{n+1}^\dagger a_n e^{imvt} \Big] + \text{H.c.}, \quad (16)$$

where $\kappa_{1,n} = \lambda_{n+1} - \lambda_n$. When the first kind of Bessel function takes the zeroth order ($m = 0$), the system possesses resonant partial NNN hopping. The Hamiltonian is simplified as

$$H_D = \sum_n [-G_n a_n^\dagger b_n + G_{n+1} a_{n+1}^\dagger b_n + T J_0(\kappa_{1,n}) a_{n+1}^\dagger a_n] + \text{H.c.}, \quad (17)$$

where $T J_0(\kappa_{1,n})$ represents the effective partial NNN hopping strength regulated by the Bessel function. The multiresonator optomechanical system can be regarded as a standard SSH chain when the parameters satisfy $J_0(\kappa_{1,n}) = 0$ and $-G_n < G_{n+1}$. We stress that the condition $\lambda_{n+1} = \lambda_n$ means that $J_0(\kappa_{1,n}) = 1$ corresponds to a nonregulated partial NNN hopping. However, the realistic selection of parameters may include relative fluctuations, thus $J_0(\kappa_{1,n}) \neq 0$ corresponds to a regulated partial NNN hopping.

Mapping of the topological SSH model based on a 1D multiresonator optomechanical system provides a new kind of optical platform for investigation of various effects of topology on other physics, such as the block of topological edge states on quantum walks. As shown in Fig. 4, we investigate the influences of topological edge states and partial NNN hopping on quantum walks. The numerical results reveal that the appearance of topological edge states will have a suppressive effect on quantum walks in the present system, as shown in Figs. 4(a) and 4(b). However, when partial NNN hopping is introduced into the system, we find that the existence of partial NNN hopping will destroy the suppression of the topological edge states on quantum walks with an increase in the partial NNN hopping strength, as shown in Figs. 4(c)–4(f). The reason is that the large partial NNN interactions will accelerate the process of quantum walks in the bulk.

More specifically, when the parameter satisfies $-G_n < G_{n+1}$ (topologically nontrivial), the topological left edge state has a maximal suppressive effect on quantum walks corresponding to $T J_0(\kappa_{1,n}) = 0$. The two degenerate zero-energy modes are separated accompanied by a decrease in the distribution of the left edge state when mild partial NNN hopping ($T J_0(\kappa_{1,n}) < -G_n$) is added in the system, which leads to a weak suppressive effect of the left edge state on quantum walks, as shown in Fig. 5(a). With the strength of the partial NNN hopping continuously increasing, the distribution of the left edge state decreases continuously while the distribution of the second site increases gradually, which further weakens the suppressive effect of the left edge state on quantum walks. A phase transition occurs when the partial NNN hopping strength reaches the same value as the strength of the NN hopping, G_{n+1} ($T J_0(\kappa_{1,n}) = G_{n+1}$), in which the first cavity field and the second resonator have the same distributions, as shown in Fig. 5(b). The reason for this phenomenon is that the first cavity field and the second resonator will be

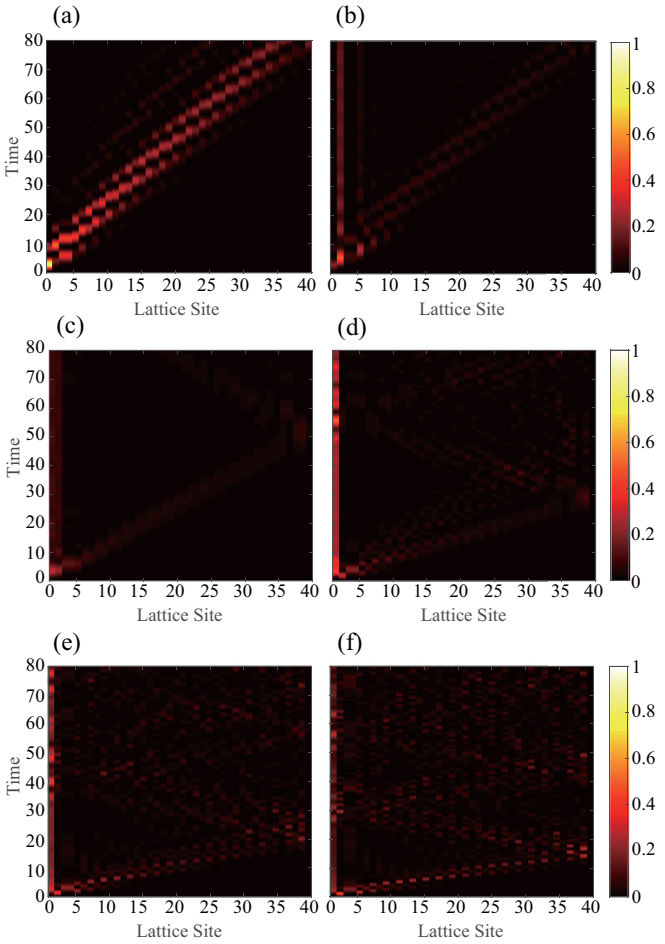

FIG. 4. Effects of the topological edge state and the partial NNN hopping on quantum walks. (a) Quantum walks in a nontopological multiresonator optomechanical system ($-G_n > G_{n+1}$). (b) Quantum walks suppressed by topological edge states ($-G_n < G_{n+1}$). (c–f) The suppression of topological edge states is destroyed by the partial NNN hopping. Strengths of the partial NNN hopping are $TJ_0(\kappa_{1,n}) =$ 0.1 (c), 0.45 (d), 0.75 (e), and 1 (f). The size of the system is $L = 40$.

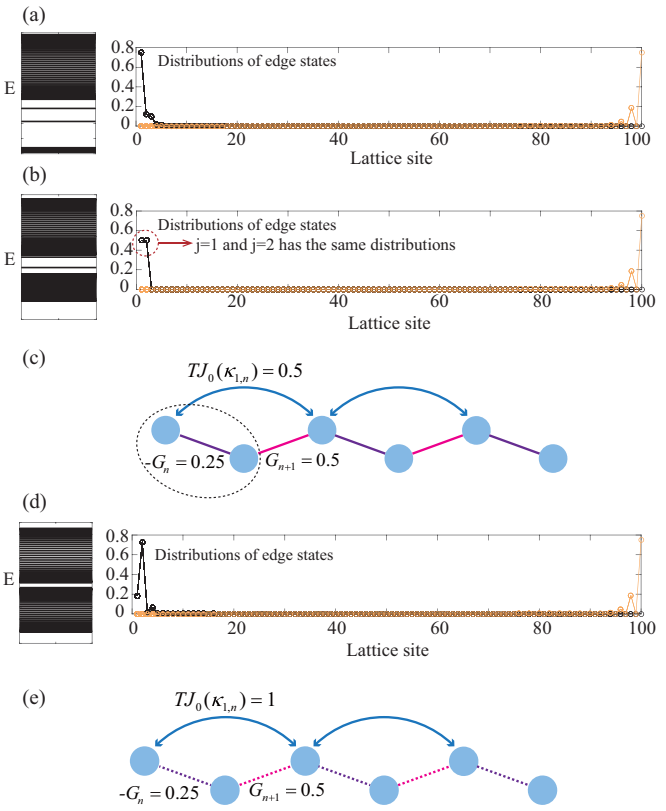

FIG. 5. Energy spectra and distributions of edge states. (a) Energy spectrum and distributions of edge states corresponding to $TJ_0(\kappa_{1,n}) = 0.25$. (b) Energy spectrum and distributions of edge states corresponding to $TJ_0(\kappa_{1,n}) = 0.5$. (c) Schematic of the multiresonator optomechanical system when the partial NNN coupling satisfies $TJ_0(\kappa_{1,n}) = G_{n+1} = 0.5$. The dashed black circle represents the supersite. (d) Energy spectrum and distributions of edge states corresponding to $TJ_0(\kappa_{1,n}) = 1$. (e) Schematic of the multiresonator optomechanical system under the large partial NNN coupling limit $TJ_0(\kappa_{1,n}) = 1$. Dashed lines represent the decoupling due to $TJ_0(\kappa_{1,n}) \gg G_{n+1}$. The quantum walk mainly passes though the odd sites (path indicated by blue arrows). Other parameters are set at $-G_n = 0.25$ and $G_{n+1} = 0.5$. The size of the system is $L = 100$.

equivalent to a supersite due to the same effective hopping strength, $TJ_0(\kappa_{1,n}) = G_{n+1}$, as shown in Fig. 5(c). This means that quantum walks can pass though the lattice in terms of two paths (the path indicated by blue arrows and the path indicated by pink lines, respectively) with the same probability at the same time. Subsequently, the distribution of the second site rises continuously with a sequential increase in the partial NNN hopping strength, and a high enough partial NNN hopping strength $[TJ_0(\kappa_{1,n}) \gg G_{n+1}]$ will separate the second sites from the lattice chain, which generates a new localized state, as shown in Fig. 5(d). A large enough partial NNN hopping limit means that quantum walks will pass though the lattice only in terms of the odd sites, which leads to the acceleration of quantum walks and destroys the suppressive effect of the left edge state on quantum walks due to the disappearance of the left edge state, as shown in Fig. 5(e). These results demonstrate that we can realize the controllable suppression and acceleration of quantum walks based on the present cavity optomechanical system with frequency modulations.

IV. CONCLUSIONS

In conclusion, we have proposed a scheme to induce a topological SSH phase via distinguishing parameter regimes based on a 1D multiresonator cavity optomechanical system with frequency modulations. We find that, after the Stokes heating terms are eliminated, the optomechanical chain system will exhibit a topological SSH phase upon variation of the effective NN hopping assisted by the frequency modulations alternately. The property of the Bessel function guarantees the realization of the SSH model corresponding to the arbitrary effective optomechanical coupling strength in a certain range. Another parameter regime is proposed to remove the resonant Stokes heating terms, in which the optomechanical chain system exhibits an SSH phase via changing of the effective optomechanical coupling alternately. We also realize a bosonic

Kitaev model with trivial topology by keeping the Stokes heating terms. Our scheme provides a controllable method for investigating the effect of partial NNN hopping in the SSH model based on a 1D multiresonator cavity optomechanical system with frequency modulations.

ACKNOWLEDGMENTS

This work was supported by the National Natural Science Foundation of China under Grants No. 61822114, No. 11874132, and No. 61575055 and the Project of Jilin Science and Technology Development for Leading Talent of Science and Technology Innovation in Middle and Young and Team Project under Grant No. 20160519022JH.

APPENDIX A: DISCUSSION OF THE FINAL TIME-DEPENDENT STEADY CAVITY FIELD

Now we give a phenomenological analysis of the final time-dependent steady cavity field due to the existence of frequency modulations. For simplicity, we focus on a tiny component of the optomechanical array, which is composed of two cavity fields and one resonator. After performance of the quantum Langevin equations, the mean values of the cavity field and mechanical resonator can be described by

$$\begin{aligned}
\dot{\alpha}_{a,1} &= -i\Delta'_{a,1}\alpha_{a,1} - \frac{\epsilon_1}{2}\alpha_{a,1} - i\Omega_1 - i\lambda_1\nu\cos(\nu t)\alpha_{a,1},\\
\dot{\beta}_{b,1} &= -i\omega_{b,1}\beta_{b,1} - \frac{\Gamma}{2}\beta_{b,1} + ig(|\alpha_{a,1}|^2 - |\alpha_{a,2}|^2)\\
&\quad - i\gamma_1\nu\cos(\nu t)\beta_{b,1},\\
\dot{\alpha}_{a,2} &= -i\Delta'_{a,2}\alpha_{a,2} - \frac{\epsilon_2}{2}\alpha_{a,2} - i\Omega_2 - i\lambda_2\nu\cos(\nu t)\alpha_{a,2},
\end{aligned} \tag{A1}$$

where ϵ_1 [ϵ_2] and Γ are the decay of the cavity field and the damping of the resonator, and $\Delta'_{a,1} = \Delta_{a,1} - g(\beta^*_{b,1} + \beta_{b,1})$ [$\Delta'_{a,2} = \Delta_{a,2} + g(\beta^*_{b,1} + \beta_{b,1})$] is the effective detuning of the cavity field. We simulate the evolutions of the cavity fields and the resonator with the time numerically, as shown in Figs. 6(a) and 6(b). The numerical results show that the two final steady cavity fields have the same periodically time-dependent steady distributions due to the existence of frequency modulations, hence the effective optomechanical coupling G_n (G_{n+1}) is also periodically time dependent. According to the above numerical results, we find that the effective optomechanical coupling can be formally written as $|-G_n| = g(A + B\cos\omega t) = A' + B'\cos\omega t$ after keeping only the dominant contribution of the Fourier-series expansion of the periodically time-dependent cavity fields, in which $A' \approx 0.91\omega_{b,1}$ and $B' \approx 0.09\omega_{b,1}$. Besides the periodically time-dependent steady cavity field, we find that the steady resonator is also periodically time dependent, hence the effective detuning of the cavity field $\Delta'_{a,1}$ ($\Delta'_{a,2}$) is time dependent. However, we find that the parameter satisfies $\Delta_{a,1} \gg g(\beta^*_{b,1} + \beta_{b,1})$ [$\Delta_{a,2} \gg g(\beta^*_{b,1} + \beta_{b,1})$], which leads to $\Delta'_{a,1} \approx \Delta_{a,1}$ ($\Delta'_{a,2} \approx \Delta_{a,2}$). In this way, the correlation between $\Delta'_{a,1}$ ($\Delta'_{a,2}$) and the time t can also be removed. Thus, the red-detuning condition can be achieved approximately with $\Delta'_{a,1} \approx \omega_{b,1}$.

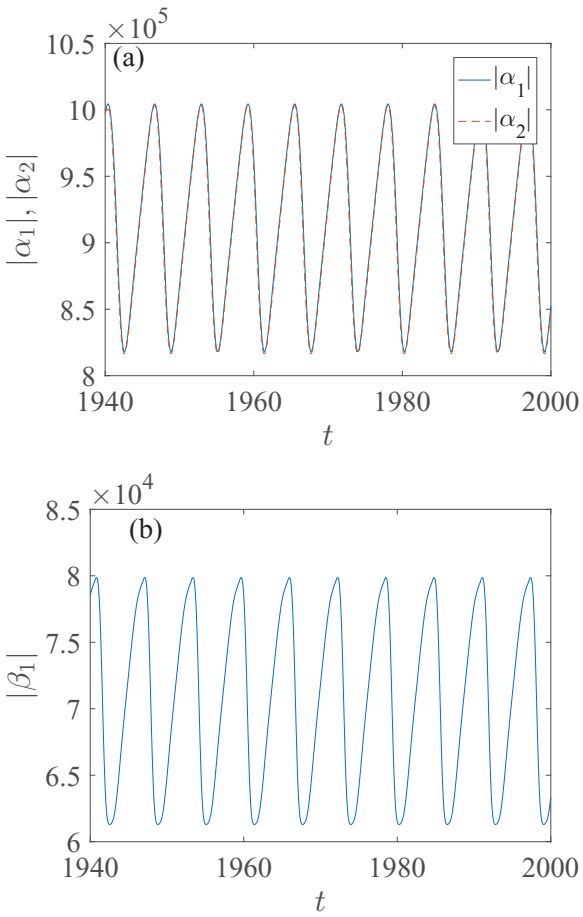

FIG. 6. Evolution of (a) the steady cavity fields and (b) the steady resonator with time. Other parameters are set at $\Delta_{a,1} = \Delta_{a,2} = \omega_{b,1}$, $\epsilon_1 = \epsilon_2 = 0.1\omega_{b,1}$, $\Gamma = 1 \times 10^{-6}\omega_{b,1}$, $\Omega_1 = \Omega_2 = 1 \times 10^5\omega_{b,1}$, $g = 2 \times 10^{-6}\omega_{b,1}$, $\lambda_1 = 1.2\omega_{b,1}$, $\lambda_2 = \gamma_1 = \omega_{b,1}$, and $\nu = \omega_{b,1}$.

APPENDIX B: LINEARIZING THE SYSTEM HAMILTONIAN CORRESPONDING TO AN EVEN NUMBER OF LATTICE SITES

Here, we consider the frequency-modulated optomechanical array composed of N cavity fields and N resonators (the lattice size is $2N$, corresponding to an even number), in which the coupling between the resonator b_n and the adjacent cavity field a_n (a_{n+1}) is g_n. The system can be described by

$$\begin{aligned}
H_{\text{even}} = \sum_{n=1}^{N}\{&[\omega_{a,n} + \lambda_n\nu\cos(\nu t + \phi)]a_n^\dagger a_n + (\Omega_n a_n^\dagger e^{-i\omega_{d,n}t} + \Omega_n^* a_n e^{i\omega_{d,n}t}) + [\omega_{b,n} + \gamma_n\nu\cos(\nu t + \phi)]b_n^\dagger b_n\\
&- g_n a_n^\dagger a_n(b_n^\dagger + b_n)\} + \sum_{n=1}^{N-1} g_n a_{n+1}^\dagger a_{n+1}(b_n^\dagger + b_n).
\end{aligned} \tag{B1}$$

Under the condition of strong laser driving, we perform the standard linearization approach to linearize the Hamiltonian. After dropping the notation "δ" for all the fluctuation operators δa_n (δb_n), the Hamiltonian can be deformed as

$$H_L = \sum_{n=1}^{N} \{[\Delta'_{a,n} + \lambda_n \nu \cos(\nu t + \phi)] a_n^\dagger a_n + [\omega_{b,n} + \gamma_n \nu \cos(\nu t + \phi)] b_n^\dagger b_n - g_n(\alpha_n^* a_n + \alpha_n a_n^\dagger)(b_n^\dagger + b_n)\} + \sum_{n=1}^{N-1} g_n(\alpha_{n+1}^* a_{n+1} + \alpha_{n+1} a_{n+1}^\dagger)(b_n^\dagger + b_n), \tag{B2}$$

where $\Delta'_{a,n}$ contains $\Delta'_{a,1} = \Delta_{a,1} + g_1(\beta_1^* + \beta_1)$ and $\Delta'_{a,n=2\ldots N} = \Delta_{a,n} - g_{n-1}(\beta_{n-1}^* + \beta_{n-1}) + g_n(\beta_n^* + \beta_n)$. After performance of a rotating transformation on the linearization Hamiltonian in Eq. (B2) with

$$V = \exp\left\{\sum_{n=1}^{N} -i\Delta'_{a,n} t a_n^\dagger a_n - i\lambda_n \sin(\nu t + \phi) a_n^\dagger a_n - i\omega_{b,n} t b_n^\dagger b_n - i\gamma_n \sin(\nu t + \phi) b_n^\dagger b_n\right\}, \tag{B3}$$

the Hamiltonian becomes

$$H'_L = \sum_{n=1}^{N} \{-G_n a_n^\dagger b_n e^{i[(\Delta'_{a,n} - \omega_{b,n})t + (\lambda_n - \gamma_n)\sin(\nu t + \phi)]} - G_n a_n^\dagger b_n^\dagger e^{i[(\Delta'_{a,n} + \omega_{b,n})t + (\lambda_n + \gamma_n)\sin(\nu t + \phi)]}\} + \sum_{n=1}^{N-1} \{G_{n+1} a_{n+1}^\dagger b_n e^{i[(\Delta'_{a,n+1} - \omega_{b,n})t + (\lambda_{n+1} - \gamma_n)\sin(\nu t + \phi)]} + G_{n+1} a_{n+1}^\dagger b_n^\dagger e^{i[(\Delta'_{a,n+1} + \omega_{b,n})t + (\lambda_{n+1} + \gamma_n)\sin(\nu t + \phi)]}\} + \text{H.c.}, \tag{B4}$$

where $G_n = g_n \alpha_n$ ($G_{n+1} = g_n \alpha_{n+1}$) is the effective optomechanical coupling parameter. Obviously, the above Hamiltonian has the same form as the Hamiltonian in Eq. (4). Thus, our scheme is also valid for the case of an even number of lattice sites. To avoid the tedious expression of two summation symbols in Eq. (B4), in the text we focus on the case of an odd number of lattice sites.

APPENDIX C: DISCUSSION ABOUT THE RATIONALITY OF THE MODULATED FREQUENCY

As revealed in Ref. [25], the frequency ν of the frequency modulations should be much higher than the effective optomechanical coupling with $\nu \gg G_n$ to ensure the rationality of removing the other heating sidebands. As mentioned in Appendix A, a typical choice of the single-photon optomechanical coupling usually is of the order of 10^{-6}, which means that the final effective optomechanical coupling G_n satisfies $G_n \sim 10^{-1}$. Then, when the modulated frequency is $\nu = \omega_b$, there seems to be an order-of-magnitude difference between the effective optomechanical coupling G_n and the modulated frequency ν. We stress that, although there is an order-of-magnitude difference, the condition $\nu \gg G_n$ is not satisfied very well. However, we can always find a parameter regime to optimize the satisfaction of this condition. For example, when we increase the decay of the cavity fields, we find that the final steady cavity fields decrease, as shown in Fig. 7(a). In this way, we can realize the condition $\nu \gg G_n$ better.

Meanwhile, as obtained in Ref. [25], the condition of a large enough ν can also be achieved via $\nu = x\omega_{b,n}$, with x being multiples of the resonator frequency, in which we can always find a set of parameters m_2 (m_4) to guarantee the existence of minimal detuning and the neglect of other heating sidebands. For example, when the modulated frequency is $\nu = 2\omega_b$, we find that the amplitudes of the two final steady cavity fields take an order in the approximate range of 10^4–10^5, as shown in Fig. 7(b). Together with the extremely weak single-photon optomechanical coupling (of the order of 10^{-6}), the final effective optomechanical coupling G_n satisfies $[G_n \sim 10^{-2}] - [G_n \sim 10^{-1}]$, so the condition $G_n \ll \nu$ is better satisfied. Especially, when $\nu = 4\omega_b$, we find that the amplitudes of the two final steady cavity fields both take order 10^4, as shown in Fig. 7(c). In this way, we have $G_n \sim 10^{-2}$ and $G_n \ll \nu$, which further optimizes the condition of $\nu \gg G_n$.

Note that the final steady cavity fields are also affected by external strong laser driving. As for an extremely strong laser driving limit, the driving field can indeed guarantee that the final steady cavity fields are large enough that the condition $G_n \ll \nu$ is invalid. However, due to the properties of the optomechanical system an extremely strong laser driving limit may destroy the stability of the system conversely. For example, when the amplitudes of the laser driving take order 10^7, we find that the amplitudes of the two cavity fields take order 10^6, as shown in Fig. 7(d). Indeed, the effective optomechanical coupling now satisfies $G_n \sim 1$ ($G_n \sim \nu$) with $\nu = \omega_b$, which means that the condition $G_n \ll \nu$ is not valid. However, at the same time, extremely strong laser driving also destroys the stability of the system, thus the two final cavity fields cannot enter steady states. This means that the strong laser driving needs to be chosen appropriately; driving that is too mild cannot ensure implementation of the linearization process, while extremely strong driving may destroy the stability of the system. Stated thus, the rationality of the condition $G_n \ll \nu$ can be assured. In the text, for simplicity, we focus on the case of $\nu = \omega_b$ to avoid the complexity caused by the different parameter regimes.

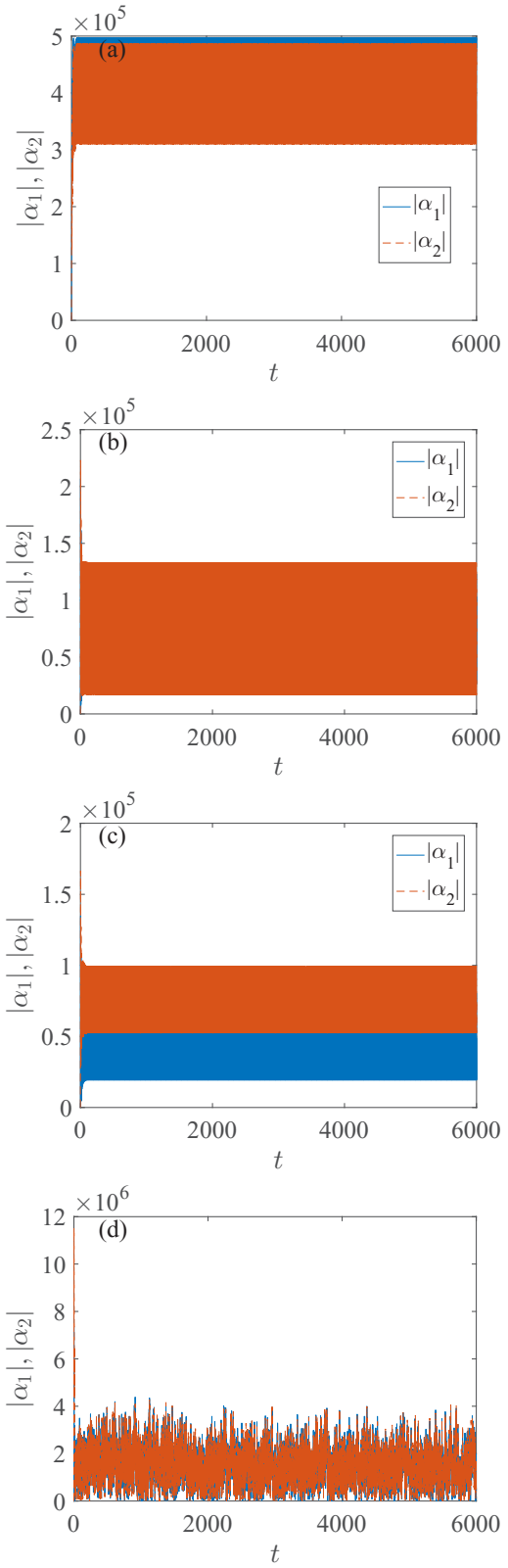

FIG. 7. Evolution of the two steady cavity fields with time. (a) $\nu = \omega_b$, (b) $\nu = 2\omega_b$, and (c) $\nu = 4\omega_b$. Other parameters are set at $\Delta_{a,1} = \Delta_{a,2} = \omega_{b,1}$, $\epsilon_1 = \epsilon_2 = 0.25\omega_{b,1}$, $\Gamma = 1 \times 10^{-6}\omega_{b,1}$, $\Omega_1 = \Omega_2 = 1 \times 10^5\omega_{b,1}$, $g = 1 \times 10^{-6}\omega_{b,1}$, $\lambda_1 = 1.5\omega_{b,1}$, and $\lambda_2 = \gamma_1 = \omega_{b,1}$. (d) $\Omega_1 = \Omega_2 = 1 \times 10^7\omega_{b,1}$ and other parameters are the same as in (a)–(c).

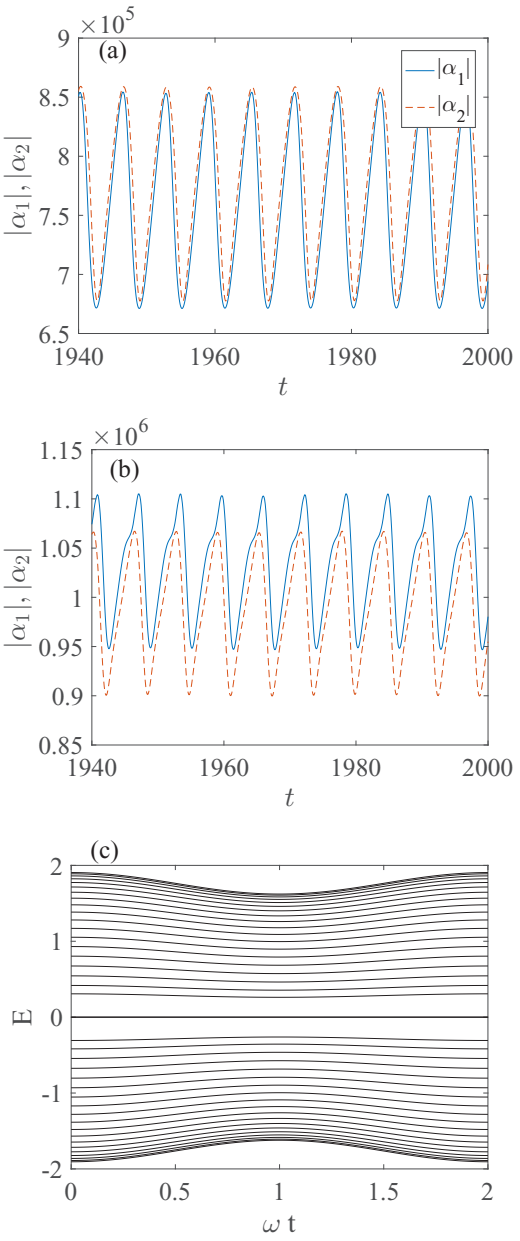

FIG. 8. Evolution of $|\alpha_{a,1}|$ (a) and $|\alpha_{a,2}|$ (b) with time. (a) $\lambda_1 = 1.6\omega_{b,1}$, $\lambda_2 = \gamma_1 = \omega_{b,1}$. (b) $\lambda_1 = 2\omega_{b,1}$, $\lambda_2 = \gamma_1 = \omega_{b,1}$. (c) Energy spectrum of the system when $|\alpha_{a,1}| > |\alpha_{a,2}|$. Other parameters are set at $\Delta_{a,1} = \Delta_{a,2} = \omega_{b,1}$, $\epsilon_1 = \epsilon_2 = 0.1\omega_{b,1}$, $\Gamma = 1 \times 10^{-6}\omega_{b,1}$, $\Omega_1 = \Omega_2 = 1 \times 10^5\omega_{b,1}$, $g = 2 \times 10^{-6}\omega_{b,1}$, and $\nu = \omega_{b,1}$.

APPENDIX D: EFFECT OF TIME-DEPENDENT EFFECTIVE OPTOMECHANICAL COUPLING ON THE TOPOLOGY OF THE SYSTEM

As mentioned in Appendix A, when the cavity fields have the same steady distributions, the effective optomechanical couplings satisfy $|-G_n| = |G_{n+1}| = A' + B'\cos\omega t$, which leads to the final effective tight-binding Hamiltonian in Eq. (7) becoming

$$H = \sum_n [J_0(\kappa_{1,n})A' + J_0(\kappa_{1,n})B'\cos\omega t]a_n^\dagger b_n + [J_0(\kappa_{3,n})A' + J_0(\kappa_{3,n})B'\cos\omega t]a_{n+1}^\dagger b_n + \text{H.c.} \quad \text{(D1)}$$

Obviously, the time-dependent fluctuations caused by the frequency modulation are equivalent to the fluctuations added in the NN hopping of the tight-binding model if we have $|J_0(\kappa_{1,n})A'| > |J_0(\kappa_{1,n})B'|$ and $|J_0(\kappa_{3,n})A'| > |J_0(\kappa_{3,n})B'|$. In this way, mild fluctuation has no effect on the topology of the system due to the protection of the energy gap. We stress that the parameters chosen in Fig. 6 make the Bessel coefficients satisfy $J_0(\kappa_{1,n}) < J_0(\kappa_{3,n})$. Theoretically, when $|J_0(\kappa_{1,n})| < |J_0(\kappa_{3,n})|$, the system always has two degenerate zero-energy modes in the gap since the effective hopping satisfies $|J_0(\kappa_{1,n})A'| < |J_0(\kappa_{3,n})A'|$ (after ignoring the effects of the time-dependent fluctuations). This means that we can always find a set of parameters to ensure the topology of the system.

To further clarify the effect of the final time-dependent steady cavity fields on the topology of the system, we focus on two more general cases, $|-G_n| < |G_{n+1}|$ and $|-G_n| > |G_{n+1}|$, as shown in Figs. 8(a) and 8(b). As shown in Fig. 8(a), the system has $|-G_n| = A'_1 + B'_1 \cos\omega t$ and $|G_{n+1}| = A'_2 + B'_2 \cos\omega t$ with $A'_1 < A'_2$ and $B'_1 < B'_2$. After ignoring the time-dependent fluctuations, we still have $|J_0(\kappa_{1,n})A'_1| < |J_0(\kappa_{3,n})A'_2|$, with $|J_0(\kappa_{1,n})| < |J_0(\kappa_{3,n})|$ under the parameter regime shown in Fig. 8(a). This means that the system also has two degenerate zero-energy modes in the gap.

Especially, as shown in Fig. 8(b), we find that the parameters satisfy $|-G_n| = A'_1 + B'_1 \cos\omega t$ and $|G_{n+1}| = A'_2 + B'_2 \cos\omega t$ with $A'_1 \approx 1.025\omega_{b,1}$, $B'_1 \approx 0.077\omega_{b,1}$, $A'_2 \approx 0.98\omega_{b,1}$, and $B'_2 \approx 0.084\omega_{b,1}$. Obviously, we have $|-G_n| > |G_{n+1}|$, which corresponds to the trivial topology in the usual tight-binding model. However, the parameters in Fig. 8(b) ensure that the Bessel coefficients satisfy $|J_0(\kappa_{1,n})| \approx 0.77\omega_{b,1}$ and $|J_0(\kappa_{3,n})| \approx \omega_{b,1}$, which means that the final effective hopping terms satisfy $|J_0(\kappa_{1,n})A'_1| < |J_0(\kappa_{3,n})A'_2|$. Thus, the system can still have two degenerate zero-energy modes in the gap, as shown in Fig. 8(c).

Based on the results mentioned above, we find that the final time-dependent steady cavity fields can have no effect on the topology of the system, which means that we can always find a set of parameters to ensure the nontrivial topology of the system. Dramatically, the topologically nontrivial phase can be achieved even when $|-G_n| > |G_{n+1}|$. We stress that the present time-dependent topological phase shown in Fig. 8(c) is actually a two-dimensional Chern topological phase. In the text, to clarify the feasibility conveniently, we treat the final time-dependent effective optomechanical coupling G_n (G_{n+1}) as an ensemble to avoid the complexity caused by different parameter regimes. For example, we choose $-G_n$ and G_{n+1} to be positive, real, and fixed values throughout the text.

[1] T. J. Kippenberg and K. J. Vahala, Cavity optomechanics: Back-action at the mesoscale, Science **321**, 1172 (2008).

[2] I. Favero and K. Karrai, Optomechanics of deformable optical cavities, Nat. Photon. **3**, 201 (2009).

[3] D. Vitali, S. Gigan, A. Ferreira, H. Böhm, P. Tombesi, A. Guerreiro, V. Vedral, A. Zeilinger, and M. Aspelmeyer, Optomechanical Entanglement Between a Movable Mirror and a Cavity Field, Phys. Rev. Lett. **98**, 030405 (2007).

[4] C. Genes, D. Vitali, and P. Tombesi, Emergence of atom-light-mirror entanglement inside an optical cavity, Phys. Rev. A **77**, 050307 (2008).

[5] W. Nie, Y. Lan, Y. Li, and S. Zhu, Generating large steady-state optomechanical entanglement by the action of Casimir force, Sci. China: Phys. Mech. Astron. **57**, 2276 (2014).

[6] J. M. Dobrindt, I. Wilson-Rae, and T. J. Kippenberg, Parametric Normal-Mode Splitting in Cavity Optomechanics, Phys. Rev. Lett. **101**, 263602 (2008).

[7] S. Gröblacher, K. Hammerer, M. R. Vanner, and M. Aspelmeyer, Observation of strong coupling between a micromechanical resonator and an optical cavity field, Nature **460**, 724 (2009).

[8] Q. Wu, J. Q. Zhang, J. H. Wu, M. Feng, and Z. M. Zhang, Tunable multi-channel inverse optomechanically induced transparency and its applications, Opt. Express **23**, 18534 (2015).

[9] W. Li, Y. Jiang, C. Li, and H. Song, Parity-time-symmetry enhanced optomechanically-induced-transparency, Sci. Rep. **6**, 31095 (2016).

[10] K. Jähne, C. Genes, K. Hammerer, M. Wallquist, E. S. Polzik, and P. Zoller, Cavity-assisted squeezing of a mechanical oscillator, Phys. Rev. A **79**, 063819 (2009).

[11] A. Kronwald, F. Marquardt, and A. A. Clerk, Dissipative optomechanical squeezing of light, New J. Phys. **16**, 063058 (2014).

[12] W. J. Gu and G. X. Li, Squeezing of the mirror motion via periodic modulations in a dissipative optomechanical system, Opt. Express **21**, 20423 (2013).

[13] W. J. Gu, G. X. Li, and Y. P. Yang, Generation of squeezed states in a movable mirror via dissipative optomechanical coupling, Phys. Rev. A **88**, 013835 (2013).

[14] P. Zhang, Y. Wang, and C. Sun, Cooling Mechanism for a Nanomechanical Resonator by Periodic Coupling to a Cooper Pair Box, Phys. Rev. Lett. **95**, 097204 (2005).

[15] X. Wang, S. Vinjanampathy, F. W. Strauch, and K. Jacobs, Ultraefficient Cooling of Resonators: Beating Sideband Cooling with Quantum Control, Phys. Rev. Lett. **107**, 177204 (2011).

[16] D. Wilson, V. Sudhir, N. Piro, R. Schilling, A. Ghadimi, and T. J. Kippenberg, Measurement-based control of a mechanical oscillator at its thermal decoherence rate, Nature **524**, 325 (2015).

[17] A. Mari and J. Eisert, Gently Modulating Optomechanical Systems, Phys. Rev. Lett. **103**, 213603 (2009).

[18] Y. Li, L. A. Wu, and Z. Wang, Fast ground-state cooling of mechanical resonators with time-dependent optical cavities, Phys. Rev. A **83**, 043804 (2011).

[19] A. Farace and V. Giovannetti, Enhancing quantum effects via periodic modulations in optomechanical systems, Phys. Rev. A **86**, 013820 (2012).

[20] J. Q. Liao, J. F. Huang, and L. Tian, Generation of macroscopic Schrödinger-cat states in qubit-oscillator systems, Phys. Rev. A **93**, 033853 (2016).

[21] J. Q. Liao, C. Law, L. M. Kuang, and F. Nori, Enhancement of mechanical effects of single photons in modulated two-mode optomechanics, Phys. Rev. A **92**, 013822 (2015).

[22] M. Wang, X. Y. Lü, Y. D. Wang, J. You, and Y. Wu, Macroscopic quantum entanglement in modulated optomechanics, Phys. Rev. A **94**, 053807 (2016).

[23] T. S. Yin, X. Y. Lü, L. L. Zheng, M. Wang, S. Li, and Y. Wu, Nonlinear effects in modulated quantum optomechanics, Phys. Rev. A **95**, 053861 (2017).

[24] M. Bienert and P. Barberis-Blostein, Optomechanical laser cooling with mechanical modulations, Phys. Rev. A **91**, 023818 (2015).

[25] D. Y. Wang, C. H. Bai, T. S. Liu, S. Zhang, and H. F. Wang, Optomechanical cooling beyond the quantum backaction limit with frequency modulation, Phys. Rev. A **98**, 023816 (2018).

[26] M. Ludwig and F. Marquardt, Quantum Many-Body Dynamics in Optomechanical Arrays, Phys. Rev. Lett. **111**, 073603 (2013).

[27] G. Heinrich, M. Ludwig, J. Qian, B. Kubala, and F. Marquardt, Collective Dynamics in Optomechanical Arrays, Phys. Rev. Lett. **107**, 043603 (2011).

[28] D. Chang, A. H. Safavi-Naeini, M. Hafezi, and O. Painter, Slowing and stopping light using an optomechanical crystal array, New J. Phys. **13**, 023003 (2011).

[29] H. Xiong, L. G. Si, X. Yang, and Y. Wu, Asymmetric optical transmission in an optomechanical array, Appl. Phys. Lett. **107**, 091116 (2015).

[30] A. Xuereb, C. Genes, and A. Dantan, Strong Coupling and Long-Range Collective Interactions in Optomechanical Arrays, Phys. Rev. Lett. **109**, 223601 (2012).

[31] A. H. Safavi-Naeini, T. M. Alegre, J. Chan, M. Eichenfield, M. Winger, Q. Lin, J. T. Hill, D. E. Chang, and O. Painter, Electromagnetically induced transparency and slow light with optomechanics, Nature **472**, 69 (2011).

[32] A. Tomadin, S. Diehl, M. D. Lukin, P. Rabl, and P. Zoller, Reservoir engineering and dynamical phase transitions in optomechanical arrays, Phys. Rev. A **86**, 033821 (2012).

[33] A. Xuereb, C. Genes, G. Pupillo, M. Paternostro, and A. Dantan, Reconfigurable Long-Range Phonon Dynamics in Optomechanical Arrays, Phys. Rev. Lett. **112**, 133604 (2014).

[34] G. de Moraes Neto, F. Andrade, V. Montenegro, and S. Bose, Quantum state transfer in optomechanical arrays, Phys. Rev. A **93**, 062339 (2016).

[35] U. Akram, W. Munro, K. Nemoto, and G. Milburn, Photon-phonon entanglement in coupled optomechanical arrays, Phys. Rev. A **86**, 042306 (2012).

[36] L. L. Wan, X. Y. Lü, J. H. Gao, and Y. Wu, Controllable photon and phonon localization in optomechanical Lieb lattices, Opt. Express **25**, 17364 (2017).

[37] L. Qi, Y. Xing, H. F. Wang, A. D. Zhu, and S. Zhang, Simulating Z_2 topological insulators via a one-dimensional cavity optomechanical cells array, Opt. Express **25**, 17948 (2017).

[38] Y. Xing, L. Qi, J. Cao, D. Y. Wang, C. H. Bai, W. X. Cui, H. F. Wang, A. D. Zhu, and S. Zhang, Controllable photonic and phononic edge localization via optomechanically induced kitaev phase, Opt. Express **26**, 16250 (2018).

[39] M. Tsindlekht, M. Golosovsky, H. Chayet, D. Davidov, and S. Chocron, Frequency modulation of the superconducting parallel-plate microwave resonator by laser irradiation, Appl. Phys. Lett. **65**, 2875 (1994).

[40] V. Singh, S. J. Bosman, B. H. Schneider, Y. M. Blanter, A. Castellanos-Gomez, and G. A. Steele, Optomechanical coupling between a multilayer graphene mechanical resonator and a superconducting microwave cavity, Nat. Nanotechnol. **9**, 820 (2014).

[41] F. Mei, J. B. You, W. Nie, R. Fazio, S. L. Zhu, and L. C. Kwek, Simulation and detection of photonic Chern insulators in a one-dimensional circuit-QED lattice, Phys. Rev. A **92**, 041805 (2015).

[42] F. Mei, Z. Y. Xue, D. W. Zhang, L. Tian, C. Lee, and S. L. Zhu, Witnessing topological Weyl semimetal phase in a minimal circuit-QED lattice, Quant. Sci. Technol. **1**, 015006 (2016).

[43] A. McDonald, T. Pereg-Barnea, and A. Clerk, Phase-Dependent Chiral Transport and Effective Non-Hermitian Dynamics in a Bosonic Kitaev-Majorana Chain, Phys. Rev. X **8**, 041031 (2018).